Relativistic four-component calculations of indirect nuclear spin-spin couplings with efficient evaluation of the exchange-correlation response kernel

Anežka Křístková, Stanislav Komorovsky, Michal Repisky, Vladimir G. Malkin, and Olga L. Malkina

Citation: The Journal of Chemical Physics **142**, 114102 (2015); doi: 10.1063/1.4913639
View online: http://dx.doi.org/10.1063/1.4913639
View Table of Contents: http://scitation.aip.org/content/aip/journal/jcp/142/11?ver=pdfcov
Published by the AIP Publishing

Relativistic four-component calculations of indirect nuclear spin-spin couplings with efficient evaluation of the exchange-correlation response kernel

Anežka Křístková,[1] Stanislav Komorovsky,[2] Michal Repisky,[2] Vladimir G. Malkin,[1] and Olga L. Malkina[1,3,a)]

[1]*Institute of Inorganic Chemistry, Slovak Academy of Sciences, Dúbravská cesta 9, SK-84536 Bratislava, Slovakia*

[2]*Centre for Theoretical and Computational Chemistry, University of Tromsø - The Arctic University of Norway, N-9037 Tromsø, Norway*

[3]*Department of Inorganic Chemistry, Comenius University, Bratislava, Slovakia*

(Received 4 December 2014; accepted 16 February 2015; published online 16 March 2015)

In this work, we report on the development and implementation of a new scheme for efficient calculation of indirect nuclear spin-spin couplings in the framework of four-component matrix Dirac-Kohn-Sham approach termed matrix Dirac-Kohn-Sham restricted magnetic balance resolution of identity for J and K, which takes advantage of the previous restricted magnetic balance formalism and the density fitting approach for the rapid evaluation of density functional theory exchange-correlation response kernels. The new approach is aimed to speedup the bottleneck in the solution of the coupled perturbed equations: evaluation of the matrix elements of the kernel of the exchange-correlation potential. The performance of the new scheme has been tested on a representative set of indirect nuclear spin-spin couplings. The obtained results have been compared with the corresponding results of the reference method with traditional evaluation of the exchange-correlation kernel, i.e., without employing the fitted electron densities. Overall good agreement between both methods was observed, though the new approach tends to give values by about 4%-5% higher than the reference method. On the average, the solution of the coupled perturbed equations with the new scheme is about 8.5 times faster compared to the reference method. © *2015 AIP Publishing LLC.* [http://dx.doi.org/10.1063/1.4913639]

INTRODUCTION

Heavy-element chemistry had always been a challenging area for theoretical chemistry. Nowadays, with the increasing power of computers and the progress in the development of quantum chemical programs, calculations of NMR parameters in heavy-element compounds become increasingly popular.[1–7] Since the effects of the electron correlation are often very important for qualitative prediction of these parameters and since quite often post-Hartree-Fock calculations are still too expensive, the Density Functional Theory (DFT) turned out to be the method of choice. In recent years, significant progress in the development of relativistic methods and relativistic DFT programs was made (see, for example, an excellent review of Belpassi *et al.*[8]). From treating relativistic effects with relativistic effective core potentials and/or using a perturbation theory to advanced four-component relativistic Hamiltonians, a tremendous progress had been made.

Several approaches for fully relativistic calculations of NMR shielding tensors with Gauge Including Atomic Orbitals (GIAO) and employing (exactly or approximately) the restricted magnetic balance (RMB) condition for the basis set were developed and implemented recently. The first code, where RMB was implemented and assessed in the framework of DFT, is the ReSpect program.[9,10] The implementation was later extended to GIAOs independently by Xiao *et al.*[11] in BDF code,[12] and Komorovsky *et al.*[13] in ReSpect. In BDF, an alternative approach based on the Kutzelnigg's transformation[14] facilitates the evaluation of NMR shielding tensor at the fully relativistic level.[15] Very recently, the group of Shiozaki had published their own implementation of RMB in the framework of Dirac-Coulomb-Gaunt Hamiltonian.[16] In the DIRAC program,[17] an alternative treatment of the magnetic balance condition, termed simple magnetic balance, has been proposed by the group of Saue.[18] Nowadays, efficient implementation (including extensive parallelization and specially tailored for RMB integral block such as InteRest[19]) allows one routinely to perform fully relativistic calculations of NMR shielding in large systems up to 100 atoms.[20,21]

However, fully relativistic four-component DFT calculations of NMR indirect nuclear spin-spin couplings proved to be more challenging. To the best of our knowledge, up to now there exist only two packages allowing one to perform such calculations: DIRAC with a pilot implementation (mentioned in Ref. 22) without inclusion of RMB as it was in their first implementation at the four-component Hartree-Fock level[23] and the ReSpect program.[24] Though the latter includes advanced features such as RMB and the finite gaussian-type model for the nuclear magnetic moment,[25] until recently the calculation

a)Author to whom correspondence should be addressed. Electronic mail: olga.malkin@savba.sk. Telephone: +421-2-59410422.

of spin-spin couplings with ReSpect program was much less efficient than the calculation of NMR chemical shifts. In this work, we report on the development and implementation of a new scheme for efficient calculation of indirect nuclear spin-spin couplings in the framework of four-component matrix Dirac-Kohn-Sham approach termed mDKS-RMB-RI-JK (matrix Dirac-Kohn-Sham RMB Resolution of Identity for J and K), which takes advantage of the previous RMB formalism and the density fitting (or resolution of identity RI) approach for the rapid evaluation of DFT exchange-correlation response kernels. The new approach is aimed to speedup the bottleneck in the solution of the coupled perturbed equations: evaluation of the matrix elements of the kernel of the exchange-correlation potential. A similar technique was used by Autschbach for the calculation of indirect spin-spin couplings at the two-component Zeroth-Order Regular Approximation (ZORA) framework.[26]

The paper is organized as follows. The theoretical background of the new method is given in the section titled "Theory." Details of our computations are summarized in "Computational Details" section. Benchmark calculations demonstrating the accuracy and efficiency of the new method are described in "Results and Discussion" section. This section also contains pilot applications to spin-spin couplings in XH4 (X = ^{13}C, ^{29}Si, ^{73}Ge, ^{119}Sn, ^{207}Pb) series and $CH_{4-n}(HgX)_n$ (X = Cl, Br, I, CN) series including assessment of the importance of solvent effects and comparison to available experimental data. Finally, the Conclusions are drawn in the last section.

THEORY

Throughout this paper, we use the Hartree system of atomic units if not noted otherwise. Summation over repeated indices is assumed and the following index notation is employed: $\boldsymbol{i}$, $\boldsymbol{j}$ denote occupied positive energy molecular orbitals (MOs), $\boldsymbol{a}$ unoccupied positive and negative energy MOs, $\boldsymbol{p}$, $\boldsymbol{q}$ all MOs and $\boldsymbol{\lambda}$, $\boldsymbol{\tau}$ are used for basis function indices. Cartesian directions are indexed by $\boldsymbol{u}$, $\boldsymbol{v}$. Superscripts $\boldsymbol{L}$, $\boldsymbol{S}$ denote the large and small component, respectively. If necessary, subscripts 2×2 and 4×4 are used to stress that the corresponding matrices are two- and four-component, respectively.

Let us start with the expression for the total energy in the presence of two magnetic fields due to magnetic moments of nuclei $\boldsymbol{M}$ and $\boldsymbol{N}$, within the framework of the four-component Dirac-Kohn-Sham (DKS) approach,

$$E^{(\vec{\mu}^M,\vec{\mu}^N)} = \left\langle \varphi_i^{(\vec{\mu}^M,\vec{\mu}^N)} \middle| D_{\mathrm{kin}}^{00} + D^{10} + D^{01} \middle| \varphi_i^{(\vec{\mu}^M,\vec{\mu}^N)} \right\rangle + E_{\mathrm{pot}}^{(\vec{\mu}^M,\vec{\mu}^N)}. \quad (1)$$

In the following, superscript $(\vec{\mu}^M,\vec{\mu}^N)$ will indicate dependence on the magnetic moments. The first term on the right-hand side represents the relativistic kinetic energy in the presence of magnetic moments $\vec{\mu}^M$ and $\vec{\mu}^N$ of nuclei $\boldsymbol{M}$ and $\boldsymbol{N}$, respectively,

$$D_{\mathrm{kin}}^{00} \equiv (\beta - 1_{4\times4})\, c^2 + c\vec{\alpha}\cdot\vec{p},$$
$$D^{10} \equiv \vec{\alpha}\cdot\vec{A}_{\vec{\mu}^M}, \quad D^{01} \equiv \vec{\alpha}\cdot\vec{A}_{\vec{\mu}^N}, \quad (2)$$

where $\boldsymbol{c}$ is speed of light, $\vec{p} = -i\vec{\nabla}$ is the momentum operator, and $\vec{A}_{\vec{\mu}^M}$ is the vector potential due to the magnetic moment of nucleus $\boldsymbol{M}$ (for the sake of simplicity, here a point model of the nuclear magnetic moment is assumed; derivation of the equations in case of a gaussian model for the nuclear magnetic moment can be found in (25)),

$$\vec{A}_{\vec{\mu}^M} = \frac{\vec{\mu}^M \times \vec{r}_M}{r_M^3}, \quad \vec{r}_M \equiv \vec{r} - \vec{R}_M, \quad (3)$$

where $\vec{R}_M$ is the position of nucleus $\boldsymbol{M}$. Dirac 4×4 matrices $\vec{\alpha}$ and β have the usual form,

$$\vec{\alpha} = \begin{pmatrix} 0 & \vec{\sigma} \\ \vec{\sigma} & 0 \end{pmatrix}, \quad \beta = \begin{pmatrix} \sigma_0 & 0 \\ 0 & -\sigma_0 \end{pmatrix}, \quad (4)$$

where $\sigma_0 \equiv 1_{2\times2}$, and $\vec{\sigma} = (\sigma_1,\sigma_2,\sigma_3)$ is a vector composed of Pauli matrices,

$$\sigma_1 = \begin{pmatrix} 0 & 1 \\ 1 & 0 \end{pmatrix}, \quad \sigma_2 = \begin{pmatrix} 0 & -i \\ i & 0 \end{pmatrix}, \quad \sigma_3 = \begin{pmatrix} 1 & 0 \\ 0 & -1 \end{pmatrix}. \quad (5)$$

The orbitals $\varphi_i^{(\vec{\mu}^M,\vec{\mu}^N)}$ are composed of two two-component spinors,

$$\varphi_i^{(\vec{\mu}^M,\vec{\mu}^N)} = \begin{pmatrix} \varphi_i^{L(\vec{\mu}^M,\vec{\mu}^N)} \\ \varphi_i^{S(\vec{\mu}^M,\vec{\mu}^N)} \end{pmatrix}, \quad (6)$$

where $\varphi_i^{L(\vec{\mu}^M,\vec{\mu}^N)}$ and $\varphi_i^{S(\vec{\mu}^M,\vec{\mu}^N)}$ are called the large and the small component of $\varphi_i^{(\vec{\mu}^M,\vec{\mu}^N)}$, respectively. In Eq. (1), $E_{\mathrm{pot}}^{(\vec{\mu}^M,\vec{\mu}^N)}$ is the potential energy, which includes the electron-nuclear Coulomb energy $E_{\mathrm{nuc}}^{(\vec{\mu}^M,\vec{\mu}^N)}$, the electron-electron Coulomb repulsion $E_{\mathrm{ee}}^{(\vec{\mu}^M,\vec{\mu}^N)}$ and the Kohn-Sham exchange-correlation energy $E_{\mathrm{xc}}^{(\vec{\mu}^M,\vec{\mu}^N)}$,

$$E_{\mathrm{nuc}}^{(\vec{\mu}^M,\vec{\mu}^N)} \equiv -\sum_M \int \frac{Z_M}{r_M} \rho_0^{(\vec{\mu}^M,\vec{\mu}^N)}(\vec{r})\, dV, \quad (7)$$

$$E_{\mathrm{ee}}^{(\vec{\mu}^M,\vec{\mu}^N)} \equiv \frac{1}{2}\iint \frac{\rho_0^{(\vec{\mu}^M,\vec{\mu}^N)}(\vec{r})\rho_0^{(\vec{\mu}^M,\vec{\mu}^N)}(\vec{r}')}{|\vec{r}-\vec{r}'|}\, dV\, dV', \quad (8)$$

$$E_{\mathrm{xc}}^{(\vec{\mu}^M,\vec{\mu}^N)} \equiv \int \varepsilon_{\mathrm{xc}}^{(\vec{\mu}^M,\vec{\mu}^N)} \left[\left\{ \rho_k^{(\vec{\mu}^M,\vec{\mu}^N)}(\vec{r}) \right\}_{k=0}^{3} \right] dV. \quad (9)$$

In Eq. (9), $\varepsilon_{\mathrm{xc}}^{(\vec{\mu}^M,\vec{\mu}^N)}$ is the non-collinear exchange-correlation energy density, which is a functional of the total electron density (ρ_0) as well as three components of spin-densities (ρ_1,ρ_2,ρ_3) and their gradients,

$$\rho_k^{(\vec{\mu}^M,\vec{\mu}^N)} \equiv \varphi_i^{(\vec{\mu}^M,\vec{\mu}^N)} \Sigma_k \varphi_i^{(\vec{\mu}^M,\vec{\mu}^N)}, \quad k \in \{0,1,2,3\}, \quad (10)$$

$$\Sigma_k \equiv \begin{pmatrix} \sigma_k & 0 \\ 0 & \sigma_k \end{pmatrix}. \quad (11)$$

The common way to solve the DKS equations is to expand the four-component MOs $\varphi_p^{(\vec{\mu}^M,\vec{\mu}^N)}$ in a finite set of basis functions. While the choice of basis set for the large component is rather straightforward, the selection of basis for the small component is more difficult and the relation between both basis sets is crucial to obtain sensible results. In this work, we expand the small component in RMB basis (as discussed and implemented in Refs. 10 and 24), where not only the coefficients but

also the basis functions depend explicitly on magnetic fields,

$$\varphi_p^{S(\vec{\mu}^M,\,\vec{\mu}^N)} = C_{\lambda p}^{S(\vec{\mu}^M,\vec{\mu}^N)} \chi_\lambda^{S(\vec{\mu}^M,\,\vec{\mu}^N)}, \tag{12}$$

$$\chi_\lambda^{S(\vec{\mu}^M,\,\vec{\mu}^N)} = \frac{1}{2c}(\vec{\sigma}\cdot\vec{p} + \frac{1}{c}\vec{\sigma}\cdot\vec{A}_{\vec{\mu}^M} + \frac{1}{c}\vec{\sigma}\cdot\vec{A}_{\vec{\mu}^N})\chi_\lambda, \tag{13}$$

and $\varphi_i^{L(\vec{\mu}^M,\,\vec{\mu}^N)}$ as a linear combination,

$$\varphi_p^{L(\vec{\mu}^M,\,\vec{\mu}^N)} = C_{\lambda p}^{L(\vec{\mu}^M,\,\vec{\mu}^N)}\,\chi_\lambda, \tag{14}$$

where $\{\chi\}$ is a common magnetic field-independent atomic basis set.

NMR indirect spin-spin coupling tensor $\mathbf{J}^{MN}$ is proportional to the reduced indirect spin-spin coupling tensor $\mathbf{K}^{MN}$ (here written in the International System of Units),

$$\mathbf{J}^{MN} = h\frac{\gamma_M}{2\pi}\frac{\gamma_N}{2\pi}\mathbf{K}^{MN}. \tag{15}$$

Above, γ_M and γ_N represent gyromagnetic ratios of the coupled nuclei $\boldsymbol{M}$ and $\boldsymbol{N}$, respectively, and $\boldsymbol{K}^{MN}$ is defined as the second derivative of the electronic energy with respect to nuclear magnetic moments $\vec{\mu}^M$ and $\vec{\mu}^N$,

$$K_{uv}^{MN} = \left.\frac{d^2E^{(\vec{\mu}^M,\vec{\mu}^N)}}{d\mu_u^M d\mu_v^N}\right|_{\vec{\mu}^M=\vec{\mu}^N=0}. \tag{16}$$

Assuming that the higher-order effects of nuclear magnetic moments are small, we will use the second-order perturbation theory for the calculation of indirect nuclear spin-spin coupling tensor. In the equations below, the superscripts $[(00),(10)_u^M$, and $(01)_v^N]$ denote the order of response with respect to the magnetic moments of nuclei M and N, respectively. The bilinear derivative of energy (Eq. (1)) can be expressed as

$$K_{uv}^{MN} = \left\langle \varphi_i^{(10)_u^M} \middle| D^{(01)_v^N} \middle| \varphi_i^{(00)} \right\rangle + \left\langle \varphi_i^{(00)} \middle| D^{(01)_v^N} \middle| \varphi_i^{(10)_u^M} \right\rangle, \tag{17}$$

where

$$\varphi_i^{(10)_u^M} = \left.\frac{d\varphi_i^{(\vec{\mu}^M,\vec{\mu}^N)}}{d\mu_u^M}\right|_{\vec{\mu}^M=\vec{\mu}^N=0},$$

$$D^{(01)_v^N} = \left.\frac{dD^{01}}{d\mu_v^N}\right|_{\vec{\mu}^M=\vec{\mu}^N=0}. \tag{18}$$

The linear response spinor $\varphi_i^{(10)_u^M}$ is the key point in the calculation of second-order properties. Since in the RMB ansatz, the four-component MO depends on magnetic fields both via MO coefficients and basis functions, we get partitioning of the response MO into regular $\varphi_i^{r(10)_u^M}$ and magnetic $\varphi_i^{m(10)_u^M}$ part,

$$\varphi_i^{(10)_u^M} \equiv \varphi_i^{r(10)_u^M} + \varphi_i^{m(10)_u^M}, \tag{19}$$

where

$$\varphi_i^{r(10)_u^M} \equiv \begin{pmatrix} C_{\lambda i}^{L(10)_u^M}\chi_\lambda \\ C_{\lambda i}^{S(10)_u^M}\chi_\lambda^{S(00)} \end{pmatrix},$$

$$\varphi_i^{m(10)_u^M} \equiv \begin{pmatrix} 0 \\ C_{\lambda i}^{S(00)}\chi_\lambda^{S(10)_u^M} \end{pmatrix}, \tag{20}$$

$$\chi_\lambda^{S(00)} \equiv \frac{1}{2c}\vec{\sigma}\cdot\vec{p}\,\chi_\lambda, \quad \chi_\lambda^{S(10)_u^M} \equiv \frac{1}{2c^2}\left[\frac{\vec{r}_M\times\vec{\sigma}}{r_M^3}\right]_u\chi_\lambda. \tag{21}$$

For $\varphi_i^{r(10)_u^M}$, the perturbed coefficients for both the large and small components are needed. Since the unperturbed atomic orbital basis covers the same space as the unperturbed MOs, we can expand the regular part of response spinor (19) in the basis of unperturbed MOs,

$$\varphi_i^{r(10)_u^M} = \beta_{pi}^{Mu}\varphi_p^{(00)}, \tag{22}$$

where index $\boldsymbol{p}$ runs over occupied as well as all unoccupied (positive- and negative-energy) MOs.

Since the detailed derivation of equations for matrix DKS method in the framework of RMB basis set (mDKS-RMB) was discussed elsewhere,[24] below we will summarize only the final equations. For the sake of simplicity, in the following, we will employ the shorthand notation $C_{\lambda i}^{L(00)} = \mathbf{C}_i^L$ and $C_{\lambda i}^{S(00)} = \mathbf{C}_i^S$. For the beta coefficients indexed by occupied indices, we obtain the following:

$$\left(\beta_{ij}^{Mu}\right)^* + \beta_{ji}^{Mu} = -\begin{pmatrix}\mathbf{C}_j^{L\dagger} & \mathbf{C}_j^{S\dagger}\end{pmatrix}\begin{pmatrix}0 & 0\\ 0 & \frac{1}{2c^2}\tilde{\Lambda}_{\mu_u^M}^P\end{pmatrix}\begin{pmatrix}\mathbf{C}_i^L\\ \mathbf{C}_i^S\end{pmatrix}, \tag{23}$$

where

$$\left(\tilde{\Lambda}_{\mu_u^M}^P\right)_{\lambda\tau} \equiv \frac{1}{2c}\left\langle\chi_\lambda\middle|\left[\frac{\vec{r}_M\times\vec{\sigma}}{r_M^3}\right]_u\vec{\sigma}\cdot\vec{p}\middle|\chi_\tau\right\rangle + \text{h.c.} \tag{24}$$

For the β_{ai}^{uM} coefficients, we obtain the following:

$$\beta_{ai}^{Mu} = \left(\varepsilon_i^{(00)} - \varepsilon_a^{(00)}\right)^{-1}\begin{pmatrix}\mathbf{C}_a^{L\dagger} & \mathbf{C}_a^{S\dagger}\end{pmatrix}\begin{pmatrix}\Re^{\text{xc, L, }Mu} & \tilde{\Lambda}_{\mu_u^M}^P\\ \tilde{\Lambda}_{\mu_u^M}^P & \Re^{\text{xc, S, }Mu} - \tilde{\Lambda}_{\mu_u^M}^P - \frac{\varepsilon_i^{(00)}}{2c^2}\tilde{\Lambda}_{\mu_u^M}^P\end{pmatrix}\begin{pmatrix}\mathbf{C}_i^L\\ \mathbf{C}_i^S\end{pmatrix}, \tag{25}$$

where $\varepsilon_i^{(00)}$ are unperturbed one-electron energies. Contributions from the exchange-correlation kernel $\Re^{\text{xc, L, }Mu}$ and $\Re^{\text{xc, S, }Mu}$,

$$\left(\Re^{\text{xc, L, }Mu}\right)_{\lambda\tau} \equiv \left.\frac{d^2E_{\text{xc}}^{(\vec{\mu}^M,\,\vec{\mu}^N)}}{d\mu_u^M dP_{\tau\lambda}^{LL}}\right|_{\vec{\mu}^M=\vec{\mu}^N=0},$$

$$\left(\Re^{\text{xc, S, }Mu}\right)_{\lambda\tau} \equiv \left.\frac{d^2E_{\text{xc}}^{(\vec{\mu}^M,\,\vec{\mu}^N)}}{d\mu_u^M dP_{\tau\lambda}^{SS}}\right|_{\vec{\mu}^M=\vec{\mu}^N=0}, \tag{26}$$

depend on the response of spin densities (and their gradients),

$$\rho_k^{(10)_u^M} = \varphi_i^{(00)\dagger}\Sigma_k\varphi_i^{(10)_u^M} + \text{c.c.}, \quad k\in\{1,2,3\}, \tag{27}$$

and thus are responsible for the coupled character of the Eq. (25). Unperturbed MOs $\varphi_i^{(00)}$ and one-electron energies $\varepsilon_i^{(00)}$ are solutions of mDKS-RKB equations (for more details see, for example, Ref. 10). In Eq. (26), $\mathbf{P}^{LL} \equiv \mathbf{C}_i^L\mathbf{C}_i^{L\dagger}$

and $\mathbf{P}^{SS} \equiv \mathbf{C}_i^S \mathbf{C}_i^{S\dagger}$ are density matrices for large and small component, respectively.

Since the iterative procedure for β_{ai}^{Mu} coefficients is the time-determining step, it is highly desirable to decrease the computational cost of kernel matrix elements evaluation. For this purpose, we will take advantage of the ideas of Dunlap[27] and Laikov,[28] who proposed to use the density expansion obtained from the robust and variational Coulomb fitting for the representation of exchange-correlation functional. The approach has already been extended to the four-component DFT case by Belpassi *et al.*[29] Here, however, we have investigated the possibility to adopt the idea of Laikov also for the calculation of second-order molecular properties in the formalism of non-collinear four-component DFT. Below, we will discuss only those parts of the scheme proposed in Ref. 28, which will illustrate the scaling properties of the approach and non-collinear form of the exchange-correlation functional.

The starting point of the present mDKS-RMB-RI-JK method is the expansion of electron density ($k = 0$) and spin-densities ($k = 1,2,3$) as linear combinations of atom-centered *auxiliary* (or *fitting*) functions $\{\xi\}$, giving approximate density $\tilde{\rho}_k$,

$$\tilde{\rho}_k(\vec{r}) = d_{k\gamma}\xi_\gamma(\vec{r}) \approx \rho_k(\vec{r}). \tag{28}$$

The fitting coefficients $d_{k\gamma}$ are obtained by minimizing the density residue,

$$\min_{\mathbf{d}}(\rho_k - \tilde{\rho}_k|\rho_k - \tilde{\rho}_k), \tag{29}$$

subject to the constraint of charge and spin conservation,

$$\forall k \in \{0,1,2,3\} \quad (\rho_k) = (\tilde{\rho}_k),$$
$$\text{where } (\,) \text{ denotes integral over } \mathbb{R}^3. \tag{30}$$

In the case of the Coulomb metric applied, the resulting fitting coefficients are calculated as follows:

$$d_{k\gamma} = (\gamma|\tau)^{-1}[(\tau|\rho_k) + \lambda_k(\tau)], \tag{31}$$

which involves the calculation of classical Coulomb integrals, denoted here as $(\,|\,)$, as well as the Lagrange multiplier of the imposed constraint,

$$\lambda_k = \frac{(\rho_k) - (\tau)(\tau|\eta)^{-1}(\eta|\rho_k)}{(\tau)(\tau|\eta)^{-1}(\eta)}, \tag{32}$$

where γ, τ, η denote fitting functions. The approximate density is then used for robust fit of the Coulomb potential[30] in the absence of the magnetic fields and the approximate exchange-correlation energy density $\tilde{\varepsilon}_{\mathrm{xc}}$ in both the absence and presence of magnetic fields (for the sake of simplicity, we omit here the explicit dependence of the exchange-correlation energy density on the gradients of electron density and spin density),

$$\tilde{\varepsilon}_{\mathrm{xc}} \equiv \varepsilon_{\mathrm{xc}}\left[\tilde{\rho}^{\pm}(\vec{r})\right], \quad \tilde{\rho}^{\pm}(\vec{r}) = \tilde{\rho}_0 \pm |\tilde{\rho}|,$$
$$|\tilde{\rho}| \equiv \sqrt{\tilde{\rho}_1^2 + \tilde{\rho}_2^2 + \tilde{\rho}_3^2}. \tag{33}$$

As a consequence, we get approximate exchange-correlation energy $\tilde{E}_{xc}$ and approximate exchange-correlation potential, taken (in the matrix formulation) as the derivative of the exchange-correlation energy with respect to density matrix,

$$\left(\tilde{V}_{\mathrm{xc}}\right)_{\lambda\tau} = \frac{d\tilde{E}_{\mathrm{xc}}}{dP_{\tau\lambda}}, \quad \mathbf{P} \equiv \mathbf{C}\mathbf{C}^{\dagger}. \tag{34}$$

After expanding the approximate electron density and spin-densities using fitting coefficients $d_{k\gamma}$ and fitting functions ξ_γ, $\tilde{V}_{\mathrm{xc}}$ is obtained in the form,

$$\left(\tilde{V}_{\mathrm{xc}}\right)_{\lambda\tau} = \frac{dd_{k\gamma}}{dP_{\tau\lambda}} \int \tilde{v}_{\mathrm{xc}}^k \left[\{\tilde{\rho}_k(\vec{r})\}_{k=0}^3\right] \xi_\gamma(\vec{r}) dV,$$
$$k \in \{0,1,2,3\}. \tag{35}$$

In Eq. (31),

$$\tilde{v}_{\mathrm{xc}}^{\pm} \equiv \frac{\delta\tilde{\varepsilon}_{\mathrm{xc}}}{\delta\tilde{\rho}^{\pm}}, \quad \tilde{v}_{\mathrm{xc}}^{0} \equiv \frac{1}{2}\left(\tilde{v}_{\mathrm{xc}}^{+} + \tilde{v}_{\mathrm{xc}}^{-}\right),$$
$$\tilde{v}_{\mathrm{xc}}^{l} \equiv \frac{1}{2}\left(\tilde{v}_{\mathrm{xc}}^{+} - \tilde{v}_{\mathrm{xc}}^{-}\right)\frac{\tilde{\rho}_l}{|\tilde{\rho}|}, \quad l \in \{1,2,3\}. \tag{36}$$

Note that in the absence of the magnetic fields and for the ground state obeying the time reversal symmetry spin-densities, $\tilde{\rho}_l$ are zero; therefore, $\tilde{v}_{\mathrm{xc}}^l$ vanishes. However, in the presence of magnetic fields, it is not true anymore and spin-densities are crucial in calculation of kernel matrix elements (Eq. (26)). In this work, matrix elements of the exchange-correlation kernel (26) are calculated using symmetric numeric derivative of matrix elements of the exchange-correlation potential (Eq. (35)).

Let us compare the computational cost of approaches with and without the density fitting applied to the exchange-correlation kernel elements. In the computational scheme employing fitting, Eq. (35), the term $\int \tilde{v}_{\mathrm{xc}}^k \xi_\gamma(\vec{r})dV$ is independent on atomic basis functions and is, therefore, calculated only once. Its computational cost is $N_{\mathrm{GP}}N_{\mathrm{AF}}$, where N_{AF} is the size of fitting basis and N_{GP} is the number of points of the numerical integration grid. The vector of these integrals (containing $4\mathrm{x}N_{\mathrm{AF}}$ elements) is then contracted with $\frac{dd_{k\gamma}}{dP_{\tau\lambda}}$ on the fly when evaluating the Coulomb integrals to save computational time. The computational cost of the calculation of the matrix elements of the approximate exchange-correlation potential is $N_{\mathrm{AF}}N_{\mathrm{AO}}^2$, where N_{AO} is the number of atomic basis functions.

On the other hand, the conventional approach (for simplicity, we will consider only large-large block),

$$\left(V_{\mathrm{xc}}^L\right)_{\lambda\tau} = \left\langle \chi_\lambda \left| v_{\mathrm{xc}}^k \right| \chi_\tau \right\rangle, \tag{37}$$

where for every unique pair of λ, τ, we have to go over N_{GP} operations (we integrate over all grid points) yields $N_{\mathrm{GP}}N_{\mathrm{AO}}^2$. Given that in most cases, $N_{\mathrm{GP}} \gg N_{\mathrm{AF}}$, we can see that using fitted kernel is promising considerable speedup of the whole calculation.

The final expression for the reduced indirect spin-spin coupling tensor can be written as follows:

$$K_{uv}^{MN} \equiv K_{uv}^{D,MN} + K_{uv}^{P0,MN} + K_{uv}^{P1,MN}, \tag{38}$$

where

$$K_{uv}^{D,MN} = \left\langle \varphi_i^{m(10)_u^M} \left| D^{(01)_v^N} \right| \varphi_i^{(00)} \right\rangle + \left\langle \varphi_i^{(00)} \left| D^{(01)_v^N} \right| \varphi_i^{m(10)_u^M} \right\rangle, \tag{39}$$

$$K_{uv}^{P0,MN} = \left[\left(\beta_{ij}^{Mu}\right)^* + \beta_{ji}^{Mu}\right] \left\langle \varphi_i^{(00)} \left| D^{(01)_v^N} \right| \varphi_j^{(00)} \right\rangle, \tag{40}$$

$$K_{uv}^{P1,MN} = 2Rel\left\{\beta_{ai}^{Mu} \left\langle \varphi_i^{(00)} \left| D^{(01)_v^N} \right| \varphi_a^{(00)} \right\rangle\right\}. \tag{41}$$

In this work, we have implemented both approaches for

evaluating the matrix elements of the exchange-correlation kernel. The conventional (fitting-free) option will serve as a benchmark method, allowing us to control the errors introduced into exchange-correlation term by density-fitting and to estimate the gain in the computational time.

Terminology

In what follows, we will use "exact kernel" as a shorthand expression for "exchange-correlation kernel without density-fitting," in contrast to "approximate kernel," which will stand for "exchange-correlation kernel obtained with density-fitting." It should be understood that our "exact" approach is far from being exact in the physical and mathematical meaning of the word.

COMPUTATIONAL DETAILS

Geometries

For the XH_4 (X = C, Si, Ge, Sn, and Pb) series (Tables I and II), we used the same geometries as in Ref. 24. For the XH series (X = F, Cl, Br, and I), the internuclear distances were taken the same as in Ref. 31. For the series $\{CH_{4-n}(HgX)_n\}$ (X = Cl, Br, I, and CN), the geometries were taken from Ref. 32. For species in Table 5, the geometry optimization in presence of 2 solvent molecules has been carried on a few chosen species at the B3LYP/MWB level, using the Gaussian 03 program package.[33]

Exchange-correlation functionals

We have used either the local density approximation with Slater exchange and VWN correlation[34] (termed SVWN) or the Generalized Gradient Approximation (GGA) functionals of Becke exchange[35] with Perdew correlation[36] functional (termed BP86), and Perdew-Burke-Ernzerhof exchange-correlation functional (termed PBE).[37] Derivatives of exchange-correlation potential were taken numerically. The step for numerical derivation of kernel has been 10^{-3} and 10^{-6} for fitted and exact kernels, respectively.

TABLE I. Comparison of the calculated $^1J(X–H)$ [Hz] in this work with results obtained by different methods and experimental data in XH_4 (X = ^{13}C, ^{29}Si, ^{73}Ge, ^{119}Sn, ^{207}Pb) series.

Method	CH_4	SiH_4	GeH_4	SnH_4	PbH_4
NR[a]	121.2	−195.9	−80.0	−1241.4	1242.4
Sc. ZORA[b]	133.3	−172.7	−74.9	−1584.5	2398.7
mDKS-RMB[a]	122.0	−201.6	−90.4	−1742.2	2345.3
This work	121.0	−198.7	−96.5	−1742.9	2495.2
Expt.	120.1[c]	−201.1[d]	−97.6[e]	−1933.3[f]	2594; 2794[g]

[a]Reference 24.
[b]Reference 44.
[c]Reference 45.
[d]Reference 46.
[e]Reference 47.
[f]Reference 48.
[g]Values estimated in Refs. 49 and 50 on the basis of experimental values for methyl-substituted plumbanes.

TABLE II. Comparison of the $^2J(H–H)$ [Hz] calculated in this work with results obtained by different methods and experimental data in XH_4 (X = ^{13}C, ^{29}Si, ^{73}Ge, ^{119}Sn, ^{207}Pb) series.

Method	CH_4	SiH_4	GeH_4	SnH_4	PbH_4
NR[a]	−13.39	−0.89	5.41	4.47	7.00
Sc. ZORA[b]	−7.62	2.36	6.08	13.94	34.23
mDKS-RMB[a]	−13.50	−0.56	7.79	14.30	30.87
This work	−13.34	−1.33	6.66	13.06	36.44
Expt.	−12.40[c]	2.75[c]	7.69[d]	15.3[c]	...

[a]Reference 24.
[b]Reference 44.
[c]Reference 52.
[d]Reference 53.

Orbital basis sets

We have used fully uncontracted Gaussian-type orbital basis sets of triple-zeta quality. For light elements (H, C, N, O, F, Si, and Cl), we employed the uncontracted polarization-consistent basis set of Jensen,[38] that have been specifically designed for calculation of spin-spin coupling constants at the HF or DFT level of theory. We also need to mention another basis set of Jensen[38] (termed pc-2), which was used for generating the auxiliary basis (see the next paragraph) for light atoms. For heavy elements (Ge, Br, Ag, Cd, Sn, I, Au, Hg, Tl, and Pb), the bases used were those of Dyall.[39] For elements Cu and Zn, where Dyall's bases were not available, we used triple-zeta Balabanov-Peterson basis.[40] The final sizes of atomic bases were [8s3p2d] (H), [12s7p3d2f] (C), [12s7p3d2f] (N), [12s7p3d2f] (O), [15s11p3d2f] (Si), [15s11p3d2f] (Cl), [23s16p10d] (Ge), [23s16p10d] (Br), [28s20p13d] (Ag), [28s20p13d] (Cd), [28s21p15d] (Sn), [28s21p15d] (I), [30s24p15d10f] (Au), [30s24p15d10f] (Hg), [30s26p17d11f] (Tl), [30s26p17d11f] (Pb), [20s16p8d2f] (Cu), and [20s16p8d2f] (Zn).

Auxiliary bases

For fitting the electron density and spin densities, the auxiliary basis sets were generated from pc-2 basis[38] (for light elements) and from triple-zeta bases[39,40] (for heavy elements) in the following way: s-exponents were chosen as doubles of the s-exponents in the orbital basis; p- and d-sets (f- and g-sets) were composed of identical exponents, covering the range of p-functions (d-functions) in the orbital basis set multiplied by two. All auxiliary basis sets were modified in even-tempered manner[41] ensuring that towards the low-exponent ("flat") end of every angular momentum the ratio between exponents is constant.

Nuclear g-values

We used the following nuclear g-values: 5.585 69 for ^1H, 1.404 82 for ^{13}C, −1.110 58 for ^{29}Si, −0.195 44 for ^{73}Ge, −2.094 56 for ^{119}Sn, 1.185 17 for ^{207}Pb, −0.566 38 for ^{15}N, 5.257 74 for ^{19}F, 0.547 92 for ^{35}Cl, 1.513 71 for ^{81}Br, 1.125 31 for ^{127}I, −0.227 36 for ^{107}Ag, −1.244 60 for ^{113}Cd, 0.097 16 for ^{197}Au, 0.350 08 for ^{67}Zn, 3.276 43 for ^{205}Tl, 1.484 90 for

^{63}Cu, and 1.011 77 for ^{199}Hg. The g-values were taken from Ref. 42.

In our work, the finite-size Gaussian-type model[41] was used for both the nuclear charge and atomic moment distribution.[25] For all atoms except hydrogen, a grid of 256 radial and 110 angular points has been used. For hydrogen, we used 128 radial and 86 angular points.

All calculations were performed sequentially using Intel(R) Xeon(R) CPU@2.60 GHz processor (i.e., without parallelization).

RESULTS AND DISCUSSION

In this section, we will address three features that will enable us to evaluate the usefulness of the newly developed approach. With the exact kernel as a reference scheme, we will analyze the accuracy of the approximate kernel approach. Second, we will estimate the gain in the computational time. The last part of this section will be devoted to comparison with experimental values.

Accuracy of the new approach compared to the reference method

The use of the fitted total and spin-densities for evaluation of the matrix elements of the kernel of the exchange-correlation potential can potentially lead to less accurate results. Since we also implemented an approach without involving the fit of the electron densities, we can address this issue by comparing the results obtained with both approaches. We performed the calculations for a representative set of 63 indirect nuclear spin-spin couplings (^{1}J(H–H), ^{2}J(H–H), ^{1}J(H–X) (X = C, Si, Ge, Sn, Pb), ^{1}J(H–X) (X = F, Cl, Br, I), ^{2}J(H–Hg), ^{3}J(C–Hg), ^{1}J(C–X) (X = Zn, Cd, Tl, Hg, Cu, Au, Ag), ^{2}J(N–Cd) (X = Zn, Cd, Tl, Hg, Cu, Au, Ag), and ^{1}J(N–X) (X = Cu, Au, Ag)) employing both types of the exchange-correlation kernel. The relation between exact and fitted kernel calculation is plotted in Fig. 1. For the data underlying Fig. 1, see Table S1 in supplementary material.[43]

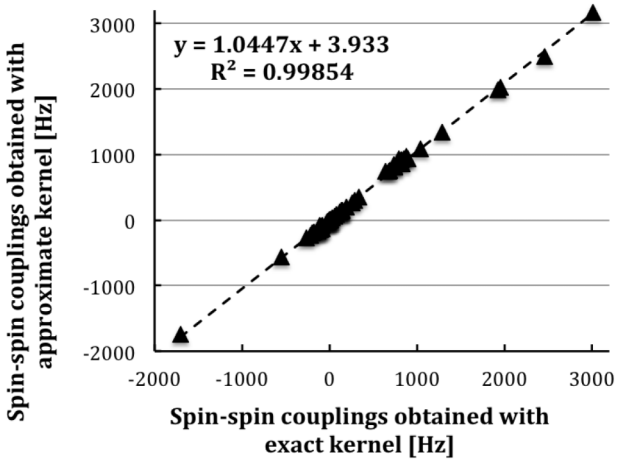

FIG. 1. Correlation between the results obtained with approximate and exact kernels. The dashed line is the linear fit for the set of points.

Given the high sensitivity of the calculated spin-spin couplings to all computational aspects, the agreement between the results obtained with approximate and exact kernels is rather good. To show more details, the central (most crowded) part of the plot is also drawn separately in Fig. S1 in supplementary material.[43] The difference between couplings is influenced by gyromagnetic values; therefore' the ratios of the corresponding counterparts have been calculated and basic statistical analysis performed on them (see Table S1 in supplementary material[43]). The average of 1.11 and median 1.04 confirms that fitted kernel gives systematically larger coupling (in absolute values). The standard deviation **σ** is equal to 0.29. We have identified an outlier ("outlier" being defined as coupling whose $\boldsymbol{J_{appr.}}/\boldsymbol{J_{exact}}$ ratio falls outside the range of $\pm 2\sigma$) ^{2}J(H–H) coupling in SiH_4, where $\boldsymbol{J_{appr}} = -1.33$ and $\boldsymbol{J_{exact}} = -0.42$. However, this coupling is the smallest from the whole set and not very relevant to the analysis based on ratios. Other near-outliers are ^{2}J(H–Hg) couplings in $CH_2(HgCl)_2$ and $CH(HgCl)_3$, having $\boldsymbol{J_{appr.}}/\boldsymbol{J_{exact}}$ ratios 1.41 and 1.57, respectively. Generally, the spin-spin couplings in halogene containing species have shown sensitivity with respect to the polarization functions in the auxiliary basis on halogene (especially bromine). It is probably connected with the presence of easily polarizable lone pairs. We have to note that in using the approximate kernel technique, the choice of the auxiliary basis for fitting electron densities is crucial: from one side, tight exponents should be sufficient to adequately fit the electron densities in the neighborhood of nuclei, and from the other side, they may lead to numerical instabilities when the fitting is done with the Coulomb metric. In the fit with the Coulomb metric, more weight is put at the valence area. When the tails of the tight exponents are adjusted for the fit in this area, the quality of the fit in the neighborhood of nuclei may suffer. One should also keep in mind that in case of GGA exchange-correlation potentials, estimation of the density gradients from the fitted total and spin densities is an additional source of losing the numerical accuracy. Therefore, the agreement between the results obtained with approximate and exact kernel in case of the local potential is much better.

Time save

Attractiveness of the fitted kernel technique lies in the time save for otherwise very demanding four-component spin-spin coupling calculation. Fig. 2 compares the time save obtained per one iteration of self-consistent field for $\beta_{ai}^{\mu_u^M}$ (onwards dubbed as β -SCF). The data, upon which the Fig. 2 is based, are available in Table S2 in supplementary material.[43]

For small systems, the time per iteration for both approaches is almost the same. However, when the number of basis functions reaches about 700 the difference became more prominent. The highest speedup can be expected (see "Theory" section) in species with high $\mathbf{N_{GP}}/\mathbf{N_{AF}}$ ratio, where $\mathbf{N_{GP}}$ is the number of grid points and $\mathbf{N_{AF}}$ is the number of auxiliary (fitting) functions. Examples are CH_4 with $\mathbf{N_{GP}}/\mathbf{N_{AF}}$ of 386.05 and $\boldsymbol{\delta_{iter}} = 42.53$, where $\boldsymbol{\delta_{iter}}$ is the ratio between the timing for one iteration in calculations with the exact and approximate kernels, respectively; HF with $\mathbf{N_{GP}}/\mathbf{N_{AF}}$ of 323.70 and $\boldsymbol{\delta_{iter}} = 32.5$; SiH_4 with $\mathbf{N_{GP}}/\mathbf{N_{AF}}$ of 323.73 and

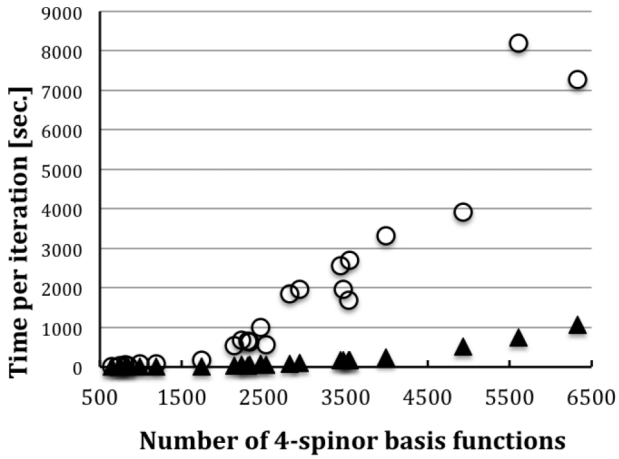

FIG. 2. Comparison of time per iteration of β-SCF. The time is given in seconds. Open circles show the time for the calculations with the exact kernel and black triangles with the approximate one. All calculations were performed sequentially using Intel(R) Xeon(R) CPU@2.60 GHz processor.

$\boldsymbol{\delta_{iter}}$ = 36.58. The opposite examples are $CH(HgCl)_3$ with $\mathbf{N_{GP}/N_{AF}}$ of 89.59 and $\boldsymbol{\delta_{iter}}$ = 7.46 or $C(HgCl)_4$ with $\mathbf{N_{GP}/N_{AF}}$ of 83.51 and $\boldsymbol{\delta_{iter}}$ = 6.78.

The average speedup for the whole calculation is about 8.5. The graph for total speedup is visually very similar to Fig. 2 and therefore not shown here (the total timings are given in Table S2 of supplementary material[43]). We have to note that the speedup gained per iteration is somewhat diminished in the total speedup. The main reason behind this is that the β_u-SCF convergence is usually slower with the approximate kernel than in the reference method. In the worst cases, the approximate kernel technique required twice more iteration to reach convergence in comparison with the reference method, but even in this case, a considerable overall speedup was achieved.

Comparison with experiment

In this part, we compare the results, obtained with the newly developed method of fitted kernel, with experimental couplings and, if possible, with another relativistic approach, namely, scalar ZORA (abbreviated as sc. ZORA). This comparison should provide some estimate where the new approach is placed among other available computational methods. At the same time, we have to note that in the present work, we were not able to use the hybrid exchange-correlation potentials employed by other authors, since the fully relativistic calculations of spin-spin couplings with hybrid functionals are undergoing a thorough testing at the moment.

XH_4 series

With reference to work of Repiský *et al.*,[24] we recalculated $^1J(H–X)$ and $^2J(H–H)$ in the benchmark series of XH_4 (X = ^{13}C, ^{29}Si, ^{73}Ge, ^{119}Sn, ^{207}Pb), employing the same geometries as in Ref. 24. The molecules of XH_4 series have well-known, well-defined geometry, little solvent effect because of the low X–H bond's polarity and the experimental data for their coupling constants are available. At the same time, X ranges from light to heavy atoms. All these make them an excellent benchmark set for a newly developed method with aspirations for relativistic spin-spin coupling. The results are collected in Tables I and II. Our results as well as the results taken from Refs. 24 and 44 were obtained with BP86 exchange-correlation functional.

As expected, for light central atom (C, Si), we get results very close to the non-relativistic case. In the whole series, our results get closer to the experiment than those obtained with scalar ZORA. The improvement is marked most notably in SnH_4 and PbH_4, where four component approach covers 92% and 93% of the experimental value, whereas scalar ZORA covers only 83% and 89%. We also have to note that in contrast to our calculations, the ZORA results were obtained with a point nucleus model. Therefore, one can expect that with a physically more realistic finite size nucleus model for the charge and magnetic moment distribution, one can expect that the ZORA values would be further decreased by about 13% for $^1J(Pb–H)$, for example.[25] From the other side, the inclusion of additional tight exponents in the basis set for a heavy element will probably yield somewhat larger value in the ZORA calculations as indicated in Ref. 51.

In the case of $^2J(H–H)$ couplings, all relativistic methods provide rather close results. We can, therefore, claim that

TABLE III. Comparison of the spin-spin couplings [Hz] calculated in this work with experimental data in $CH_{4-n}(HgX)_n$ (X = Cl, Br, I, CN). Experimental data are taken from Ref. 55 unless specified otherwise.

		^2J (^{199}Hg–H)		^1J ($^{13}CH_{4-n}$–H)		^1J (^{199}Hg–^{13}C N)		^1J (^{199}Hg–CH_{4-n})	
X	n	This work	Expt.	This work	Expt.	This work	Expt.	This work	Expt.
Cl	1	−168	±221	139	137			929	1678
	2	−142	±172	151	147			966	1782
	3	−130	±124	152	153			929	1827
	4							739	1797
Br	1	−168	±213	139[a]	139			820	1625[b]
I	1	−154	±180	138	138			758	1543[b]
CN	2	−144	±157	145	142	934	1249	811	1488
	3	−141	±127	146	165	1085	1331	744	1455
	4					1213	1428	595	

[a]Reference 56.
[b]Reference 57.

TABLE IV. Solvation effect on ^{1}J (^{199}Hg–C) [Hz] for compounds MeHgX (X = Cl, Br, I) and Hg(CN)$_2$.

		Without solvent		With two solvent molecules			
Species	Solvent	Sc. ZORA[a]	This work	Sc. ZORA[a]	This work[b]	This work	Expt.
MeHgCl	DMSO	1000.6	928.6	1415.5	954.8	1487.1	1673.8[c]
MeHgBr	DMSO	1010.9	809.7	1380.2	925.7	1466.0	1630.9[c]
MeHgI	DMSO	963.6	744.6	1364.9	840.3	1395.4	1540[c]
Hg(CN)$_2$	MeOH	2411.2	1989.7[d]	2790.2	2022.7[d]	2486.4[d]	3142.5[e]

[a]Reference 58.
[b]Geometry optimized in presence of two solvent molecules, spin-spin coupling calculations done without the two solvent molecules.
[c]Reference 59.
[d]Average from both cyano carbons.
[e]Reference 60.

spin-orbit effects for these couplings are not important. The only problematic case is the coupling in SiH_4, where our method gives different sign than scalar ZORA. Still, our result is in agreement with the value obtained with non-relativistic post-Hartree-Fock (see Ref. 54, which reports −1.45 Hz for the discussed coupling), which contradicts both scalar ZORA and experiment. We see that our new method follows the experimental values in satisfactory way, as well as the results of its predecessor.[24]

$CH_{4-n}(HgX)_n$ (X = Cl, Br, I, CN) series

For the second benchmark series, we have chosen spin-spin couplings in Hg containing compounds—$CH_{4-n}(HgX)_n$ (X = Cl, Br, I, CN). The obtained results are collected in Table III together with experimental data.

The calculated ^{1}J(C–H) spin-spin couplings are in perfect agreement with experiment. Agreement is slightly worse for ^{2}J(^{199}Hg–H) values. The calculated ^{1}J(^{199}Hg–^{13}CN) is underestimated by about 20%-30% compared to the experimental values. The worst agreement is observed for ^{1}J (^{199}Hg–CH_{4-n}), where the computed values are only about one half of the experimental ones. While certainly the deficiencies of DFT may contribute to the discrepancy, we decided to look more carefully at the experimental conditions.

Solvent effect

Experimental data given Table III were obtained in solution. To roughly estimate the environment effects on ^{1}J(Hg–C) couplings, geometry optimization in the presence of 2 solvent molecules has been carried on a HgMeX (X = Cl, Br, I) and Hg(CN)$_2$ at the B3LYP/MWB level, using the Gaussian 03[33] program package. Spin-spin couplings have then been calculated in two ways—with and without the solvent molecules. The results, compared with the ones obtained by Autschbach and Ziegler using scalar ZORA,[58] are displayed in Table IV.

In all investigated cases, the spin-spin coupling increases substantially in the presence of solvent. This effect is less pronounced in Hg(CN)$_2$. The sole geometry change contributes 6.6% of the total increase in Hg(CN)$_2$, 14.7% in MeHgI, and 17.7% in MeHgBr. Thus, in the case of investigated molecules, not only the geometry change but also donor-acceptor bonds between solvent and the coordinatively unsaturated mercury atom must be taken into account. Results obtained in this work can be compared with their ZORA[58] counterparts only loosely, as there are at least two distinctive factors. In Ref. 58, Vosko-Wilk-Nusair exchange-correlation functional[34] with X-α[61] model for the response kernel was used, while this work employs BP86. Moreover, the point nucleus model for charge distribution used in Ref. 58 is known to give systematically larger spin-spin couplings (in absolute values) than the finite model,[41] used in this work.

In this work, the solvent effect on spin-spin couplings was estimated rather approximately. For a throughout study, more solvent molecules should enter the picture (see Ref. 58) and molecular dynamics simulation should be used to describe the liquid. Still, the main conclusion—that solvent effects need to be taken into account—is well seen even in our crude model.

CONCLUSIONS

In this work, a new method for efficient calculation of indirect nuclear spin-spin couplings in context of four-component matrix Dirac-Kohn-Sham approach was presented. The new approach is aimed to speedup the bottleneck in the solution of the coupled perturbed equations: evaluation of the matrix elements of the kernel of the exchange-correlation potential. For this, the Laikov scheme[28] for using the fitted electron density for evaluations of the matrix elements of the exchange-correlation potential was extended to relativistic framework and modified for the evaluation of the matrix elements of the kernel of the exchange-correlation potential.

The new method was tested on a representative set of 63 spin-spin couplings (^{1}J(H–H), ^{2}J(H–H), ^{1}J(H–X) (X = C, Si, Ge, Sn, Pb), ^{1}J(H–X) (X = F, Cl, Br, I), ^{2}J(H–Hg), ^{3}J(C–Hg), ^{1}J(C–X) (X = Zn, Cd, Tl, Hg, Cu, Au, Ag), ^{2}J(N–X) (X = Zn, Cd, Tl, Hg, Cu, Au, Ag), and ^{1}J(N–X) (X = Cu, Au, Ag)). The obtained results were compared with the corresponding results of the reference method with traditional evaluation of the exchange-correlation kernel, i.e., without employing the fitted electron densities. Overall good agreement between both methods was observed, though the new approach tends to give values by about 4%-5% higher than the reference method. On the average, the solution of the coupled perturbed equations in the new method is about 8.5 times faster compared to the reference method. The gain in the computational time per iteration was even higher but somewhat slower convergence

damped the effect. Slower convergence is likely caused by slightly less accurate evaluation of the matrix elements of the exchange-correlation potential compared to the reference method. In some cases, higher (than average) sensitivity of the results to the choice of the auxiliary basis functions used for the fit of the electron densities is observed, that also indicates the necessity to pay special attention to the numerical aspects of the new approach.

Pilot applications of the new method to NMR spin-spin couplings in XH_4 (X = ^{13}C, ^{29}Si, ^{73}Ge, ^{119}Sn, ^{207}Pb) and HgMeX (X = Cl, Br, I) series and $Hg(CN)_2$ were performed, and the obtained results were compared to available experimental values. While for ^{1}J(C–H) and ^{2}J(H–H) in XH_4 (X = ^{13}C, ^{29}Si, ^{73}Ge, ^{119}Sn, ^{207}Pb) series generally good agreement with experiment was achieved, for the mercury containing compounds, the situation was different. The quality of the obtained results strongly depended on the type of coupling. For example, while the calculated ^{1}J(C – H) spin-spin couplings were in perfect agreement with experiment, ^{1}J(^{199}Hg–CH_{4-n}) couplings were underestimated by about 50%. To investigate the source of discrepancy, we tried at least approximately to simulate experimental conditions and include solvent effects into account. This was done by optimizing the geometry and performing additional calculations of ^{1}J(^{199}Hg–C) in HgMeX (X = Cl, Br, I) and $Hg(CN)_2$ in the presence of two solvent molecules. Even this crude model dramatically improved the agreement with experiment, in accord with the previous results of Autschbach and Ziegler using scalar ZORA.[58]

Although highly efficient parallelized method for calculations of indirect nuclear spin-spin couplings without involving the fitted electron densities within the four-component matrix Dirac-Kohn-Sham approach would be more preferable, for the time being, the new approach presents a reasonable compromise between the accuracy and computational efficiency.

ACKNOWLEDGMENTS

This work has received support from the Grant Agency of the Ministry of Education of the Slovak Republic and Slovak Academy of Sciences VEGA 2/0148/13, and from the Slovak Research and Development Agency APVV-0510-12 and APVV-0483-10. Support from the Research Council of Norway (Grant Nos. 179568 and 214095) as well as from the European Research Council through a Starting Grant (Grant No. 279619) is also gratefully acknowledged. Computational time has been provided through a grant from the Norwegian supercomputing program NOTUR (Grant No. NN4654K). We thank Dr. Taye B. Demissie for useful remarks about the manuscript.

[1]T. Helgaker, M. Jaszunski, and M. Pecul, Prog. Nucl. Magn. Reson. Spectrosc. **53**, 249 (2008).
[2]J. Autschbach and T. Ziegler, "Relativistic computation of NMR shieldings and spin–spin coupling constants," in *Encyclopedia of Nuclear Magnetic Resonance, Advances in NMR* Vol. 9, edited by D. M. Grant and R. K. Harris (John Wiley and Sons, Chichester, 2002), p. 306.
[3]J. Autschbach and T. Ziegler, "Relativistic calculations of spin–spin coupling constants of heavy nuclei," in *Calculation of NMR and EPR Parameters Theory and Applications*, edited by M. Kaupp, M. Bühl, and V. G. Malkin (Wiley–VCH, Weinheim, 2004), p. 249.
[4]M. Kaupp, "Relativistic effects on NMR chemical shifts," *Relativistic Electronic Structure Theory, Part 2: Applications*, Theoretical and Computational Chemistry Vol. 14, edited by P. Schwerdtfeger, (Elsevier, Amsterdam, 2004), p. 552.
[5]J. Autschbach, "Relativistic effects on magnetic resonance parameters and other properties of inorganic molecules and metal complexes," in *Relativistic Methods for Chemists*, Challenges and Advances in Computational Chemistry and Physics Vol. 10 edited by M. Barysz and Y. Ishikawa (Springer, 2010).
[6]J. Autschbach, "Perspective: Relativistic effects," J. Chem. Phys. **136**, 150902 (2012).
[7]T. Saue, "Relativistic Hamiltonians for chemistry: A primer," ChemPhysChem **12**, 3077 (2011).
[8]L. Belpassi, L. Storchi, and H. M. Quiney, Phys. Chem. Chem. Phys. **13**, 12368 (2011).
[9]ReSpect, version 3.4.0, 2014–Relativistic Spectroscopy DFT program of authors M. Repisky, S. Komorovsky, V. G. Malkin, O. L. Malkina, M. Kaupp, and K. Ruud, with contributions from R. Bast, U. Ekstrom, M. Kadek, S. Knecht, L. Konecny, I. Malkin Ondik, and E. Malkin, 2014, see http://rel-qchem.sav.sk.
[10]S. Komorovský, M. Repiský, O. L. Malkina, V. G. Malkin, I. Malkin Ondík, and M. Kaupp, J. Chem. Phys. **128**, 104101 (2008).
[11]L. Cheng, Y. Xiao, and W. Liu, J. Chem. Phys. **131**, 244113 (2009).
[12]W. Liu, G. Hong, D. Dai, L. Li, and M. Dolg, Theor. Chim. Acta **96**, 75 (1997).
[13]S. Komorovsky, M. Repisky, O. L. Malkina, and V. G. Malkin, J. Chem. Phys. **132**, 154101 (2010).
[14]W. Kutzelnigg, Phys. Rev. A **67**, 032109 (2003).
[15]Y. Xiao, W. Liu, L. Cheng, and D. Peng, J. Chem. Phys. **126**, 214101 (2007).
[16]R. D. Reynolds and T. Shiozaki, "Fully relativistic self-consistent field under a magnetic field," Phys. Chem. Chem. Phys. (published online).
[17]DIRAC, a relativistic *ab initio* electronic structure program, release DIRAC13, written by L. Visscher, H. J. Aa. Jensen, R. Bast, and T. Saue, with contributions from V. Bakken, K. G. Dyall, S. Dubillard, U. Ekström, E. Eliav, T. Enevoldsen, E. Faßhauer, T. Fleig, O. Fossgaard, A. S. P. Gomes, T. Helgaker, J. K. Lærdahl, Y. S. Lee, J. Henriksson, M. Iliaš, Ch. R. Jacob, S. Knecht, S. Komorovský, O. Kullie, C. V. Larsen, H. S. Nataraj, P. Norman, G. Olejniczak, J. Olsen, Y. C. Park, J. K. Pedersen, M. Pernpointner, K. Ruud, P. Sałek, B. Schimmelpfennig, J. Sikkema, A. J. Thorvaldsen, J. Thyssen, J. van Stralen, S. Villaume, O. Visser, T. Winther, and S. Yamamoto, 2013, see http://www.diracprogram.org.
[18]M. Olejniczak, R. Bast, T. Saue, and M. Pecul, J. Chem. Phys. **136**, 014108 (2012).
[19]M. Repisky, InteRest 2.0, An integral program for relativistic quantum chemistry, 2013.
[20]P. Hrobarik, V. Hrobarikova, F. Meier, M. Repisky, S. Komorovsky, and M. Kaupp, J. Phys. Chem. A **115**, 5654-5659 (2011).
[21]T. B. Demissie, M. Repisky, S. Komorovsky, J. Isaksson, J. S. Svendsen, H. Dodziuk, and K. Ruud, J. Phys. Org. Chem. **26**, 679 (2013).
[22]J. Vaara, M. Hanni, and J. Jokisaari, J. Chem. Phys. **138**, 104313 (2013).
[23]L. Visscher, T. Enevoldsen, T. Saue, H. J. A. Jensen, and J. Oddershede, J. Comput. Chem. **20**, 1262 (1999).
[24]M. Repiský, S. Komorovský, O. L. Malkina, and V. G. Malkin, Chem. Phys. **356**, 263 (2009).
[25]E. Malkin, Ph.D. thesis, Comenius University, Bratislava, 2009.
[26]J. Autschbach, J. Chem. Phys. **129**, 094105 (2008).
[27]B. I. Dunlap, J. Andzelm, and J. W. Mintmire, Phys. Rev. A **42**, 6354 (1990).
[28]D. N. Laikov, Chem. Phys. Lett. **281**, 151 (1997).
[29]L. Belpassi, F. Tarantelli, A. Sgamellotti, and H. M. Quiney, Phys. Rev. B **77**, 233403 (2008).
[30]B. I. Dunlap, J. Mol. Struct.: THEOCHEM **529**, 37 (2000).
[31]K. P. Huber and G. Herzberg, *Constants of Diatomic Molecules, Molecular Spectra and Molecular Sctructure* (Van Nostrand Reinhold, New York, 1979), Vol. 4.
[32]M. Kaupp and O. L. Malkina, J. Chem. Phys. **108**, 3648 (1998).
[33]M. J. Frisch, G. W. Trucks, H. B. Schlegel, G. E. Scuseria, M. A. Robb, J. R. Cheeseman, J. A. Montgomery, Jr., T. Vreven, K. N. Kudin, J. C. Burant, J. M. Millam, S. S. Iyengar, J. Tomasi, V. Barone, B. Mennucci, M. Cossi, G. Scalmani, N. Rega, G. A. Petersson, H. Nakatsuji, M. Hada, M. Ehara, K. Toyota, R. Fukuda, J. Hasegawa, M. Ishida, T. Nakajima, Y. Honda, O. Kitao, H. Nakai, M. Klene, X. Li, J. E. Knox, H. P. Hratchian, J. B. Cross, V. Bakken, C. Adamo, J. Jaramillo, R. Gomperts, R. E. Stratmann, O. Yazyev, A. J. Austin, R. Cammi, C. Pomelli, J. W. Ochterski, P. Y. Ayala, K. Morokuma, G. A. Voth, P. Salvador, J. J. Dannenberg, V. G. Zakrzewski, S. Dapprich, A. D. Daniels, M. C. Strain, O. Farkas, D. K. Malick, A. D. Rabuck, K. Raghavachari, J. B. Foresman, J. V. Ortiz, Q. Cui, A. G. Baboul,

S. Clifford, J. Cioslowski, B. B. Stefanov, G. Liu, A. Liashenko, P. Piskorz, I. Komaromi, R. L. Martin, D. J. Fox, T. Keith, M. A. Al-Laham, C. Y. Peng, A. Nanayakkara, M. Challacombe, P. M. W. Gill, B. Johnson, W. Chen, M. W. Wong, C. Gonzalez, and J. A. Pople, Gaussian 03, Revision C.02 (Gaussian, Inc., Wallingford, CT, 2004).
[34]S. Vosko, L. Wilk, and M. Nusair, Can. J. Phys. **58**, 1200 (1980).
[35]A. D. Becke, Phys. Rev. A **38**, 3098 (1988).
[36]J. P. Perdew, Phys. Rev. B **33**, 8822 (1986).
[37]J. P. Perdew, K. Burke, and M. Ernzerhof, Phys. Rev. Lett. **77**, 3865 (1996).
[38]F. Jensen, J. Chem. Theory Comput. **2**, 1360 (2006).
[39]K. G. Dyall, Theor. Chem. Acc. **108**, 335 (2002); **109**, 284 (2003); **115**, 441 (2006); **112**, 403 (2004).
[40]N. B. Balabanov and K. A. Peterson, J. Chem. Phys. **123**, 064107 (2005).
[41]E. Malkin, M. Repiský, S. Komorovský, P. Mach, O. Malkina, and V. Malkin, J. Chem. Phys. **134**, 044111 (2011).
[42]E. R. Cohen, T. Cvitas, J. G. Frey, B. Horey, B. Holmström, K. Kuchitsu, R. Marquardt, I. Mills, F. Pavese, M. Quack, J. Stohner, H. L. Strauss, M. Takami, and A. J. Thor, *Quantities, Units and Symbols in Physical Chemistry, IUPAC Green Book*, 3rd ed. (IUPAC & RSC Publishing, Cambridge, 2008).
[43]See supplementary material at http://dx.doi.org/10.1063/1.4913639 for data underlying Figs. 1 and 2 and the central part of the plot in Fig. 1 drawn in a different scale.
[44]I. Malkin Ondík, TZ2P basis, unpublished results done with Amsterdam Density Functional (ADF), https://www.scm.com/ADF/.
[45]W. T. Raynes, J. Geertsen, and J. Oddershede, Chem. Phys. Lett. **197**, 576 (1992).
[46]P. W. Fowler, Mol. Phys. **43**, 591 (1981).
[47]A. L. Wilkins, P. J. Watkinson, and K. M. MacKay, J. Chem. Soc., Dalton Trans. **1987**, 2365.
[48]H. Dreeskamp, Z. Naturforsch. **19a**, 139 (1964).
[49]T. Enevoldsen, L. Visscher, T. Saue, H. J. Jensen, and J. Oddershede, J. Chem. Phys. **112**, 3493 (2000).
[50]J. Autschbach and T. Zieger, J. Chem. Phys. **113**, 936 (2000).
[51]S. Moncho and J. Autschbach, J. Chem. Theor. Comput. **6**, 223 (2010).
[52]W. Bruegel, *Handbook of NMR Spectral Parameters* (Heyden, London, 1979), Vol. 13.
[53]E. Edsworth, S. G. Frankiss, and A. G. Robiette, J. Mol. Spectrosc. **12**, 299 (1964).
[54]S. Kirpekar, H. J. Aa. Jensen, and J. Oddershede, Chem. Phys. **188**, 171 (1994).
[55]W. Kress and D. K. Breitiger, J. Organomet. Chem. **246**, 1 (1983).
[56]Y. Kawasaki, M. Aritomi, and J. Iyoda, Bull. Chem. Soc. Jpn. **49**, 3478 (1976).
[57]N. K. Wilson, R. D. Zehr, and P. D. Ellis, J. Magn. Reson. **21**, 437 (1976).
[58]J. Autschbach and T. Ziegler, J. Am. Chem. Soc. **123**, 3341 (2001).
[59]A. J. Brown, O. W. Howarth, and P. Moore, J. Chem. Soc., Dalton Trans. **1976**, 1589.
[60]A. Sebald and B. Wrackmeyer, J. Magn. Reson. **63**, 397 (1985).